Improved method for hot embossing As_2S_3 waveguides employing a thermally stable chalcogenide coating

Ting Han,* Steve Madden, Sukhanta Debbarma, and Barry Luther-Davies

Centre for Ultrahigh Bandwidth Devices for Optical Systems, Laser Physics Centre, Research School of Physics and Engineering, The Australian National University, Canberra, ACT 2600, Australia
**tih111@rsphysse.anu.edu.au*

Abstract: We demonstrate the fabrication of As_2S_3 rib waveguides using hot embossing. Because of the high temperature required, a thin (50nm) $Ge_{11.5}As_{24}Se_{64.5}$ was thermally evaporated on top of an 870nm As_2S_3 layer to protect against surface degradation during embossing. The waveguides propagation loss was 0.52dB/cm for the TE and 0.41dB/cm for the TM polarizations at 1550nm for a waveguide cross-section dimension of 3.8 × 1μm. The nonlinearity of a 2.2μm wide waveguide was shown to be $13500W^{-1}km^{-1}$ using four-wave mixing demonstrating that these embossed waveguides were capable of being used for all-optical processing.

OCIS codes: (130.4310) Nonlinear; (130.2755) Glass waveguides; (190.4360) Nonlinear optics, devices.

References and links

1. C. Quémard, F. Smektala, V. Couderc, A. Barthelemy, and J. Lucas, "Chalcogenide glasses with high non linear optical properties for telecommunications," J. Phys. Chem. Solids **62**(8), 1435–1440 (2001).
2. J. M. Harbold, F. O. Ilday, F. W. Wise, J. S. Sanghera, V. Q. Nguyen, L. B. Shaw, and I. D. Aggarwal, "Highly nonlinear As-S-Se glasses for all-optical switching," Opt. Lett. **27**(2), 119–121 (2002).
3. A. Prasad, C. J. Zha, R. P. Wang, A. Smith, S. Madden, and B. Luther-Davies, "Properties of $Ge_xAs_ySe_{1-x-y}$ glasses for all-optical signal processing," Opt. Express **16**(4), 2804–2815 (2008).
4. M. D. Pelusi, V. G. Ta'eed, Libin Fu, E. Magi, M. R. E. Lamont, S. Madden, Duk-Yong Choi, D. A. P. Bulla, B. Luther-Davies, and B. J. Eggleton, "Applications of highly-nonlinear chalcogenide glass devices tailored for high-speed all-optical signal processing," IEEE J. Sel. Top. Quantum Electron. **14**(3), 529–539 (2008).
5. M. Galili, J. Xu, H. C. Mulvad, L. K. Oxenløwe, A. T. Clausen, P. Jeppesen, B. Luther-Davies, S. Madden, A. Rode, D.-Y. Choi, M. Pelusi, F. Luan, and B. J. Eggleton, "Breakthrough switching speed with an all-optical chalcogenide glass chip: 640 Gbit/s demultiplexing," Opt. Express **17**(4), 2182–2187 (2009).
6. V. G. Ta'eed, M. R. E. Lamont, D. J. Moss, B. J. Eggleton, D. Y. Choi, S. Madden, and B. Luther-Davies, "All optical wavelength conversion via cross phase modulation in chalcogenide glass rib waveguides," Opt. Express **14**(23), 11242–11247 (2006).
7. S. J. Madden, D. Y. Choi, D. A. Bulla, A. V. Rode, B. Luther-Davies, V. G. Ta'eed, M. D. Pelusi, and B. J. Eggleton, "Long, low loss etched $As_{(2)}S_{(3)}$ chalcogenide waveguides for all-optical signal regeneration," Opt. Express **15**(22), 14414–14421 (2007).
8. D. Choi, S. Madden, D. Bulla, R. Wang, A. Rode, and B. Luther-Davies, "Submicrometer-thick low-loss As_2S_3 planar waveguides for nonlinear optical devices," IEEE Photon. Technol. Lett. **22**(7), 495–497 (2010).
9. D. Choi, S. Madden, D. Bulla, R. Wang, A. Rode, and B. Luther-Davies, "Thermal annealing of arsenic tri-sulphide thin film and its influence on device performance," J. Appl. Phys. **107**(5), 053106 (2010).
10. D. Y. Choi, S. Madden, A. Rode, R. P. Wang, A. Ankiewicz, and B. Luther-Davies, "Surface roughness in plasma-etched As_2S_3 films: Its origin and improvement," IEEE Trans. Nanotechnol. **7**(3), 285–290 (2008).
11. T. Han, S. Madden, B. Luther-Davies, and R. Charters, "High-quality polarization-insensitive polysiloxane waveguide gratings produced by UV nanoimprint lithography," IEEE Photon. Technol. Lett. **22**(23), 1720–1722 (2010).
12. H. Schift, "Nanoimprint lithography: an old story in modern times? a review," J. Vac. Sci. Technol. B **26**(2), 458–480 (2008).
13. X. H. Zhang, Y. Guimond, and Y. Bellec, "Production of complex chalcogenide glass optics by molding for thermal imaging," J. Non-Cryst. Sol. **326**, 519–523 (2003).

#156486 - $15.00 USD Received 13 Oct 2011; revised 15 Nov 2011; accepted 17 Nov 2011; published 29 Nov 2011

14. W. J. Pan, H. Rowe, D. Zhang, Y. Zhang, A. Loni, D. Furniss, P. Sewell, T. M. Benson, and A. B. Seddon, "One-step hot embossing of optical rib waveguides in chalcogenide glasses," Microw. Opt. Technol. Lett. **50**(7), 1961–1963 (2008).
15. M. Solmaz, H. Park, C. K. Madsen, and X. Cheng, "Patterning chalcogenide glass by direct resist-free thermal nanoimprint," J. Vac. Sci. Technol. B **26**(2), 606–610 (2008).
16. Z. G. Lian, W. Pan, D. Furniss, T. M. Benson, A. B. Seddon, T. Kohoutek, J. Orava, and T. Wagner, "Embossing of chalcogenide glasses: monomode rib optical waveguides in evaporated thin films," Opt. Lett. **34**(8), 1234–1236 (2009).
17. T. Han, S. Madden, D. Bulla, and B. Luther-Davies, "Low loss chalcogenide glass waveguides by thermal nano-imprint lithography," Opt. Express **18**(18), 19286–19291 (2010).
18. D. Y. Choi, S. Madden, D. Bulla, R. P. Wang, A. Rode, and B. Luther-Davies, "Thermal annealing of arsenic tri-sulphide thin film and its influence on device performance," J. Appl. Phys. **107**(5), 053106 (2010).
19. X. Gai, T. Han, A. Prasad, S. Madden, D. Y. Choi, R. P. Wang, D. Bulla, and B. Luther-Davies, "Progress in optical waveguides fabricated from chalcogenide glasses," Opt. Express **18**(25), 26635–26646 (2010).
20. H. Schmid and B. Michel, "Siloxane polymers for high-resolution, high-accuracy soft lithography," Macromolecules **33**(8), 3042–3049 (2000).
21. T. Han, S. Madden, M. Zhang, R. Charters, and B. Luther-Davies, "Low loss high index contrast nanoimprinted polysiloxane waveguides," Opt. Express **17**(4), 2623–2630 (2009).
22. M. R. E. Lamont, B. Luther-Davies, D. Y. Choi, S. Madden, X. Gai, and B. J. Eggleton, "Net-gain from a parametric amplifier on a chalcogenide optical chip," Opt. Express **16**(25), 20374–20381 (2008).

Introduction

Chalcogenide glasses contain one or more of the chalcogen elements (S, Se or Te) as a major constituent covalently bonded to network formers, such as Ge, As, Ga, or Si to form a glass with unusual and sometimes remarkable properties. Chalcogenides have found widespread application as phase change materials for optical data storage media (DVD-Rs) and non-volatile random access memories (PRAM); as lens materials for infrared imaging; as photovoltaic cells; and due to their large non-resonant non-linearity and low linear and non-linear losses (see e.g. [1–3]) as promising materials for integrated devices for all-optical processing [4–6]. The wide transparency of chalcogenides (out to 20μm in some cases) has also sparked a lot of interest in their use to create integrated devices for mid-infrared sensing and defense applications since most chemical or biological contaminants or toxins have their spectral fingerprints in this region.

Chalcogenide waveguides fabricated using standard photolithography combined with dry plasma etching have been reported to have propagation losses as low as 0.05dB/cm for As_2S_3 waveguides with ~7μm^2 mode areas, and ~0.2dB/cm at 1550nm for devices with ~1.7μm^2 mode area [7]. These results were, however, not easy to achieve because chalcogenides are aggressively attacked by alkaline chemicals used during photolithography as well as most gases in plasma form. Thus, this conventional fabrication process becomes rather complex requiring the use of protective layers [8]; optimized annealing conditions prior to etching [9]; and tailored process chemistries [10].

Nanoimprint lithography is a low cost and high throughput fabrication technique requiring only a single step to fabricate a complicated optical device [11]. They are also well known for their ability to produce features on the nanometer scale [12] without use of chemical processing. Several groups have demonstrated the possibility of molding chalcogenide glasses [13–16] although there have been few demonstration of low loss waveguides using this approach.

In 2010, we demonstrated that low loss chalcogenide waveguide could be molded in a single step from $As_{24}Se_{36}S_{36}$ glass films using a simple hot-embossing apparatus and innovative soft stamp [17]. We showed that a soft, low-cost Polydimethylsiloxane (PDMS) stamp could produce waveguides with excellent surface morphology and losses as low as 0.26dB/cm at 1550nm (limited by Rayleigh scattering in the glass films). The relatively low glass transition temperature of $As_{24}Se_{36}S_{36}$ (~110°C) is an advantage for hot embossing, but the material itself is somewhat impractical for real world devices, being susceptible to crystallization under embossing conditions, and was found also to be photosensitive in optical experiments at around 1550nm.

#156486 - $15.00 USD Received 13 Oct 2011; revised 15 Nov 2011; accepted 17 Nov 2011; published 29 Nov 2011

In this paper we, therefore, describe the use of a similar embossing approach to fabricate waveguides from the more robust and optically stable As_2S_3 glass that has already been proven effective in the most demanding of applications – all-optical signal processing [4–6]. The higher glass transition temperature of this glass (≈170°C) suggests that a much higher embossing temperature is needed compared with $As_{24}Se_{36}S_{36}$. One of the first reports of experiments on embossing As_2S_3 was carried out at 225°C at a pressure of 5×10^6 Pa and although submicron structures were successfully produced, significant problems were reported due to the appearance of crystals on the embossed surfaces [15].

In fact degradation at high annealing temperatures is known to occur in evaporated As_2S_3 films. Recent experiments have shown that the surface of a thermally evaporated As_2S_3 film starts to roughen as determined by atomic force microscopy at an annealing temperature of 150°C under vacuum and increased by an order of magnitude over the as-deposited film at 170°C [18]. At a temperatures typically expected for hot embossing (>220°C), surface degradation becomes a substantial problem suggesting that hot embossing may not lead to high quality waveguides. One solution that has been explored was to use a surface coating to inhibit surface diffusion that contributes to the growth of crystals on the surface of thermally evaporated As_2S_3 films. Indeed it has been reported that a thin layer of SU8 (40nm) on top of the As_2S_3 [19] was sufficient to inhibit surface degradation at up to 300°C: ≈120°C above the glass transition temperature. However, the SU8 protective layer was found to be too rigid and resisted the deformation needed to create a well-defined rib waveguide with sharp edges.

In this paper we used a different surface treatment comprising a 50nm layer of another chalcogenide glass, $Ge_{11.5}As_{24}Se_{64.5}$ ($Ge_{11.5}$) thermally evaporated on top of the 870nm thick As_2S_3 layer. $Ge_{11.5}$ whose refractive index is 2.65 at 1550nm, has a higher glass transition temperature compared to As_2S_3, ≈210-220°C, but importantly we found that surface roughening did not occur in this material until it was heated above 270°C, close to or above the embossing temperature required for As_2S_3. In addition, by adding a hard *h*-PDMS layer on the surface of a softer PDMS stamp, we could increase the local rigidity but maintained global flexibility of the stamp thereby improving the profile of the embossed waveguides [20].

Fabrication

Films 0.87μm thick of As_2S_3 glass were deposited by thermal evaporation onto 100mm <100> silicon wafers with 1.5μm of thermal oxide as an under cladding. The deposition was carried out in a chamber evacuated to 2×10^{-7} Torr and at a source to substrate distance of ~40cm using a heated Molybdenum boat. After thermal annealing at 130°C for 24 hours, a 50nm $Ge_{11.5}$ layer was deposited on top of the As_2S_3 layer again by thermal evaporation.

A master for the stamp was etched into the thermal oxide layer on top of a silicon wafer using standard photolithography and dry etching with an Oxford Plasmalab ICP-100 and CHF_3 gas. The pattern etched 450nm deep into the oxide was then coated with a ~10nm thick PTFE anti-stick layer using plasma processing with CHF_3 gas but ICP power only on the reactor [21]. A ~10μm thick layer of *h*-PDMS solution was then spin coated on top of the master stamp and thermally cured on a hot plate. Following this, a ~1mm thick layer of PDMS was poured on top of the *h*-PDMS and cured in a vacuum oven before being peeled from the master. This stamp design offers the advantages of overall flexibility but a harder surface compared with PDMS alone and is of advantage when embossing microscopic features [20].

The As_2S_3 waveguides were fabricated using a process similar to that previously employed for $As_{24}S_{38}Se_{38}$ [17]. The embossing temperature, however, was raised to 280°C and a uniform pressure of 2 bar was applied over the entire 4 inch wafer for 5 minutes. De-molding was performed at 120°C after flash cooling the system at ~40°C/min. After embossing a 10μm thick layer of a UV-curable polysiloxane was spin-coated on top of the waveguide pattern forming the top cladding for the waveguides.

Surface crystallization is a well-know issue when a thin film of As_2S_3 is exposed to high temperatures and this is the major problem when hot embossing. An example of this

#156486 - $15.00 USD Received 13 Oct 2011; revised 15 Nov 2011; accepted 17 Nov 2011; published 29 Nov 2011

phenomenon taken by an optical microscope is shown in Fig. 1(a) where severe surface crystallization was observed after hot embossing an uncoated As_2S_3 film at 280°C. Interestingly this crystallization is less evident in the optical micrographs in regions where the highest pressure was applied to the material suggesting it is quite sensitive to surface conditions. In fact, we reported previously that surface degradation can be eliminated by bonding a stable SU8 coating to the film surface [19]. To determine whether we could substitute a more stable and flexible glass layer for this purpose we measured the surface roughness of a ≈1μm thick $Ge_{11.5}$ film, using a Veeco NT9100 optical profiler with x100 objective, as it was annealed under vacuum at increasingly higher temperatures. For this material the onset of roughening did not occur until the temperature exceeded ≈280°C.

We, therefore, added a 50nm $Ge_{11.5}$ coating on top of the As_2S_3 and this produced a dramatic improvement in the surface quality of the embossed waveguides (Figs. 1(b), 2(a)) with no evidence of surface degradation of crystallization. At 280°C, the $Ge_{11.5}$ layer was also soft enough to be easily deformed by the stamp and hence the waveguide cross-section was much sharper compared with the results obtained using a 40nm SU8 protective layer [19] (Figs. 1(c) and 1(d)). The high magnification SEM images in Fig. 2(a) confirmed that the sidewalls were very well defined with sharp corners where they connected to the horizontal surfaces and were also quite smooth. However, at lower SEM magnification (Fig. 2(b)), some rougher regions at the bottom edge of the waveguide sidewalls were just discernable and these seemed to occur periodically along the waveguide. The period of this variation is a few microns and its amplitude is approximately ± 20nm. This appears to originate from deformation of the surface of the stamp during embossing, possibly due to the underlying PDMS backing being too flexible. In spite of this the ribs are of high quality and appear good enough for optical applications including as nonlinear waveguide devices for all-optical signal processing.

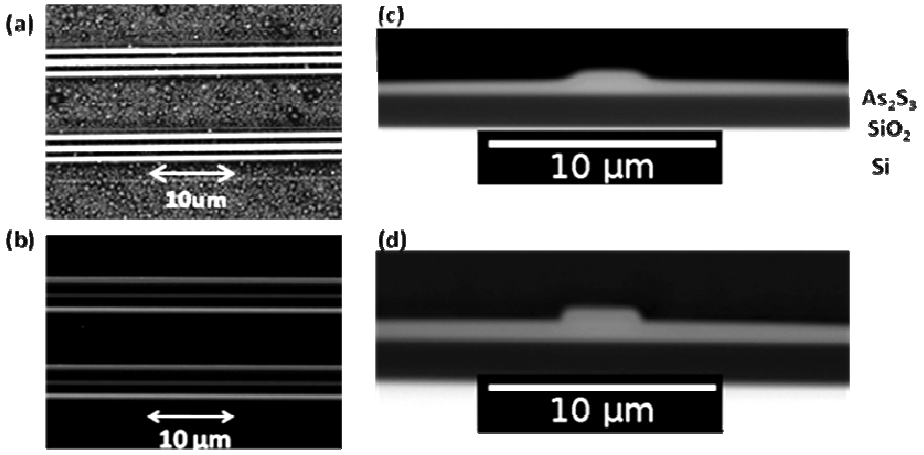

Fig. 1. Optical microscopic images of the embossed As_2S_3 waveguide showing (a) surface crystallization without protective coating; (b) no surface degradation with 50nm $Ge_{11.5}$ coating; (c) the waveguide cross-section with 40nm SU8 coating; (d) the waveguide cross section with 50nm $Ge_{11.5}$ coating.

#156486 - $15.00 USD Received 13 Oct 2011; revised 15 Nov 2011; accepted 17 Nov 2011; published 29 Nov 2011

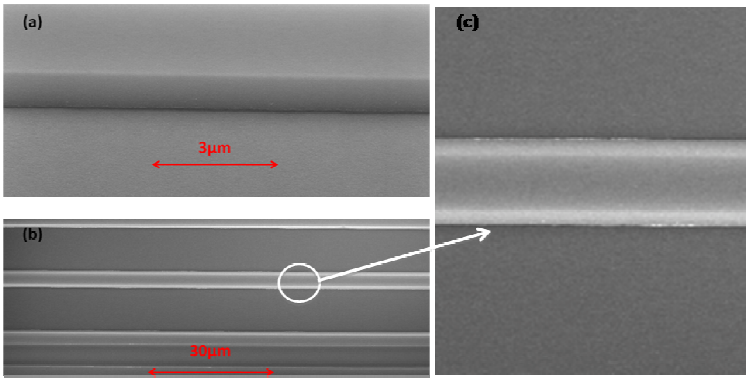

Fig. 2. SEM images of the embossed As_2S_3 waveguides. (a) side wall image at 45°; (b) plan view showing the embossed wavguide surrounded by depressed trenches; (c) magnified portion from (b) showing some roughening at the bottom of the rib.

Loss measurements

To assess their suitability as nonlinear waveguides, we first determined the optical losses at 1550nm using the cut-back method. For these measurements we first measured the total loss for an 8.3cm long waveguide before cleaving it into two samples ≈1/3 and 2/3 of the original length and re-measuring the losses. For these measurements, light from a tunable external cavity semiconductor laser was coupled into the waveguides using lensed fibers, which produced a 2.5µm $1/e^2$ mode field diameter, and the transmitted power was measured using a power meter. Because these waveguides were multimode at 1550nm, they showed significant mode coupling and beating that produced strong and random (from waveguide to waveguide) wavelength dependence of the insertion loss. The transmission was therefore determined by sweeping the laser over a ~100nm range and identifying the minimum loss over a 10pm bandwidth. Figure 3 shows the resulting cut-back results for TE and TM modes for 4 different 2.2µm wide waveguides and 7 different 3.8µm wide waveguides from a single wafer. The measurement uncertainty was found to be +/–0.1dB from repeated measurements and the values were consistent within < ± 0.5 between different samples. From these results the propagation loss for the 3.8µm waveguide was found to be 0.52dB/cm for TE and 0.41dB/cm for TM polarizations and 0.8dB/cm for TE and 0.66dB/cm for TM for the 2.2µm wide waveguides. These losses are similar to those obtained by embossing As_2S_3 with an SU8 coating as described in [19], and about double than the best values from dry etching [8].

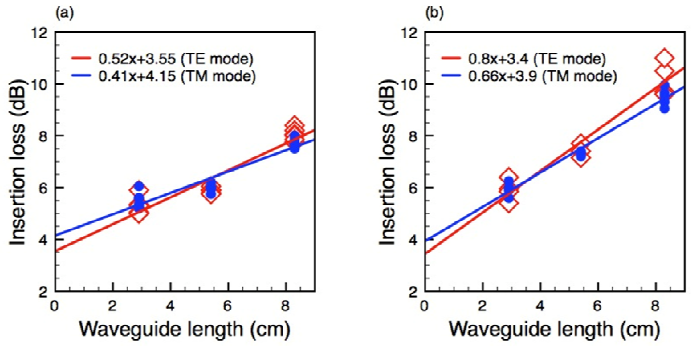

Fig. 3. Optical insertion loss of cutback measurements for nominal waveguide width of (a) 3.8µm averaged over 7 waveguides and (b) 2.2µm averaged over 4 waveguides.

#156486 - $15.00 USD Received 13 Oct 2011; revised 15 Nov 2011; accepted 17 Nov 2011; published 29 Nov 2011

The dependence of the loss over a broad wavelength range was measured by coupling a supercontinuum generated in a photonic crystal fiber driven by 10ps pulses from a mode-locked Nd:YVO_4 laser into the waveguides. The transmission between 600 and 1700nm was determined using an Agilent 86142B optical spectrum analyzer. Measurements from 8.3cm and 2.9cm long chips were used to eliminate the contribution of coupling losses from these data. The resulting normalized loss spectrum is plotted in Fig. 4. Note the small increase in absorption beyond 1600nm is caused by overtone absorption in the upper cladding.

A good fit to these data was obtained by assuming that the loss has contributions from both Rayleigh and side-wall scattering (scaling with $1/\lambda^4$ and $1/\lambda^2$ respectively). At the shortest wavelength (≈800nm), Rayleigh and side-wall scattering are approximately equal, whilst at longer wavelengths side-wall scattering becomes dominant and is 3-4 times higher than the Rayleigh component at 1550nm. This is in agreement with the results of Fig. 3 which shows the TE loss is always higher than the TM loss by about 25%, which suggests that significant contribution comes from scattering on the vertical side-walls which would more strongly affect the TE mode. This contribution to the loss may be associated with the long period side-wall ripples observable in the fabricated devices. Nevertheless, the measured losses from this simple single step embossing method are within a factor of two of the best achieved using conventional photolithography and dry etching and are low enough for even demanding applications such as optical signal processing.

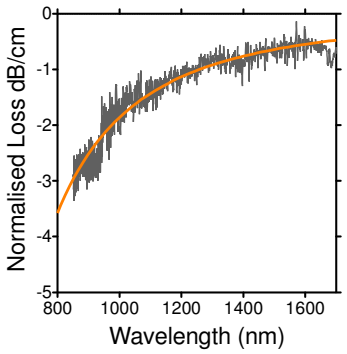

Fig. 4. Wavelength dependence of the propagation loss of the embossed waveguide.

Optical nonlinearity

The optical nonlinearity of the 8.3cm long waveguides was measured using four-wave mixing between two CW sources. Pump and signal wavelengths were generated by combining the outputs from CW lasers operating at 1550.8nm and 1552.3nm using a WDM coupler. Both signal and pump were amplified using erbium-doped fiber amplifiers (EDFAs) and band-pass filters used to attenuate any amplified spontaneous emission. The combined signals were coupled into and out of the waveguide using lensed fibres. Polarization controllers were used to adjust both pump and signal to either the TE or TM mode. A power meter was used to monitor the input power at the pump and the output spectrum was acquired using an optical spectrum analyzer and used to determine the conversion to the generated idler waves. The experimental layout is illustrated in Fig. 5(a).

The measured conversion efficiency was first confirmed to have a square relation to the pump power as shown in Fig. 5(b) indicating that competing nonlinear processes such as stimulated Brillouin Scattering (SBS) were absent at the power levels that were used. The nonlinear coefficient could then be calculated through the idler conversion efficiency based on the relation:

$$\eta = \exp(-\alpha L)(\gamma P_p L_{eff})^2$$

#156486 - $15.00 USD Received 13 Oct 2011; revised 15 Nov 2011; accepted 17 Nov 2011; published 29 Nov 2011

where P_p is the input power; α is the linear propagation loss; and η is the idler conversion efficiency at the output. The effective length L_{eff} accounts for group velocity dispersion and can be described as:

$$L_{eff} = \sqrt{1+\exp(-2\alpha L)-2\exp(-\alpha L)\cos(\Delta\beta L)} \,/\, \sqrt{\alpha^2+\Delta\beta^2}$$

where L is the waveguide length; and $\Delta\beta$ is the difference in the propagation constants at the pump and signal wavelengths. Since the wavelength separation of the pump and signal was small, $\Delta\beta \approx 0$, hence using the known values for the power at the lensed fiber, the coupling losses, the propagation losses and relative output powers, the nonlinear coefficient could be calculated to be $13500 \pm 2000 \mathrm{W^{-1}km^{-1}}$ for a 2.2μm wide waveguide which is similar to values reported for As_2S_3 waveguide made using dry etching techniques [22]. It should be noted that the height of these embossed waveguides had increased to ~1μm from the 920nm of the original film due to the buildup of the displaced of material during the hot embossing process. This needs to be taken into account if dispersion engineering is being used to obtain anomalous dispersion at the pump wavelength since the dispersion is sensitive to the waveguide thickness. It is worth noting that according to modeling, the presence of this thin $Ge_{11.5}$ layer had only a small effect on the mode profile and does not change the effective nonlinearity since this layer interacts only with the low intensity regions of the mode.

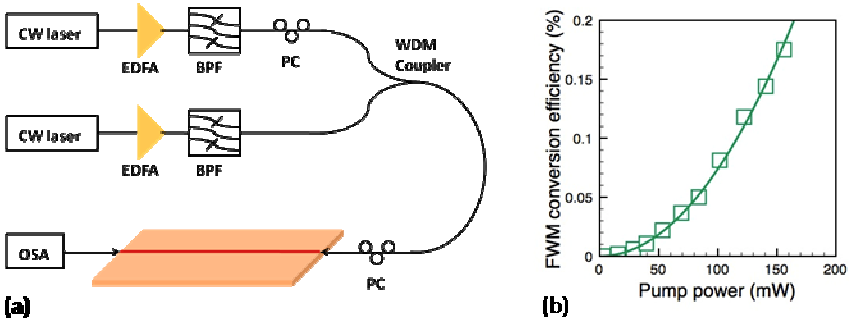

Fig. 5. (a) Experimental setup for FWM experiments; (b) measured FWM conversion efficiency versus pump power with a fit to a square law relation.

Conclusion

We have fabricated high quality low loss As_2S_3 waveguides by hot embossing. The deposition of a thin layer of $Ge_{11.5}$ chalcogenide glass successfully eliminated degradation of the surface which occurs on bare As_2S_3 films exposed to high temperatures and was sufficiently flexible to allow molding of sharp and well-defined waveguide sidewalls using a PDMS stamp with a harder *h*-PDMS surface layer. The measured loss for the embossed waveguides was as low as 0.41dB/cm for TM polarization for a 3.8μm × 1μm waveguide and appears to be limited by the long period variations in the waveguide width due to deformation of the stamp. The nonlinearity of a 2.2μm wide waveguide was measured to be $13500 \mathrm{W^{-1}km^{-1}}$ and this is sufficient for all-optical processing of telecommunications signals. This work demonstrates it is feasible to employ hot embossing to produce low loss, high quality waveguides in stable As_2S_3 glass. In particular this single step approach to waveguide fabrication can lead to the production of waveguides at low cost for applications such as disposable optical sensors.

Acknowledgments

This research was conducted by the Australian Research Council's Centre of Excellence for Ultrahigh bandwidth Devices for Optical Systems (project number CE110001018).

#156486 - $15.00 USD Received 13 Oct 2011; revised 15 Nov 2011; accepted 17 Nov 2011; published 29 Nov 2011